Supporting information

Table ST1: Comparison the $La_{1-x}Sr_xCoO_3$ perovskite oxide catalyst based aprotic Li-O_2 battery.

Catalyst	Current rate	Discharge capacity (mAh/g)	Overpotential (V)	Reference
HS $La_{0.6}Sr_{0.4}CoO_{3-\delta}$	**100 mA g^{-1}**	**4895**	**1.016**	**Present work**
$La_{0.6}Sr_{0.4}CoO_{3-\delta}$	100 mA g^{-1}	4701	1.1	R1
$La_{0.6}Sr_{0.4}CoO_{3-\delta}$	100 mA g^{-1}	3256	0.85	R2
$La_{0.6}Sr_{0.4}CoO_3$	30 mA g^{-1}	3672	~1.4	R3
$La_{0.6}Sr_{0.4}Co_{0.9}Mn_{0.1}O_3$	200 mA g^{-1}	3107	~1.4	R4
$La_{0.5}Sr_{0.5}CoO_{3-x}$ Nanotubes	25 mA g^{-1}	5799	1.14	R5
$La_{0.8}Sr_{0.2}Mn_{0.6}Ni_{0.4}O_3$	50 mA g^{-1}	5364	1.33	R6
$La_{0.4}Sr_{0.6}MnO_3$	50 mA g^{-1}	5624	1.45	R7

R1. M.Y. Oh, J.S. Jeon, J.J. Lee, P. Kim, K.S. Nahm, The bifunctional electrocatalytic activity of perovskite $La_{0.6}Sr_{0.4}CoO_{3-\delta}$ for oxygen reduction and evolution reactions, RSC Advances, 5 (2015) 19190-19198.

R2. J.J. Lee, M.Y. Oh, K.S. Nahm, Effect of Ball Milling on Electrocatalytic Activity of Perovskite $La_{0.6}Sr_{0.4}CoO_{3-\delta}$ Applied for Lithium Air Battery, Journal of The Electrochemical Society, 163 (2016) A244-A250.

R3. N. Sun, H. Liu, Z. Yu, Z. Zheng, C. Shao, The $La_{0.6}Sr_{0.4}CoO_3$ perovskite catalyst for Li-O_2 battery, Solid State Ionics, 268 (2014) 125-130.

R4. N. Sun, H. Liu, Z. Yu, Z. Zheng, C. Shao, Mn-doped $La_{0.6}Sr_{0.4}CoO_3$ perovskite catalysts with enhanced performances for non-aqueous electrolyte Li-O_2 batteries, RSC Advances, 6 (2016) 13522-13530.

R5. G. Liu, H. Chen, L. Xia, S. Wang, L.-X. Ding, D. Li, K. Xiao, S. Dai, H. Wang, Hierarchical Mesoporous/Macroporous Perovskite $La_{0.5}Sr_{0.5}CoO_{3-x}$ Nanotubes: A Bifunctional Catalyst with Enhanced Activity and Cycle Stability for Rechargeable Lithium Oxygen Batteries, ACS Applied Materials & Interfaces, 7 (2015) 22478-22486.

R6. Z. Wang, Y. You, J. Yuan, Y.-X. Yin, Y.-T. Li, S. Xin, D. Zhang, Nickel-Doped $La_{0.8}Sr_{0.2}Mn_{1-x}Ni_xO_3$ Nanoparticles Containing Abundant Oxygen Vacancies as an Optimized Bifunctional Catalyst for Oxygen Cathode in Rechargeable Lithium–Air Batteries, ACS Applied Materials & Interfaces, 8 (2016) 6520-6528.

R7. Y. Zhao, Y. Hang, Y. Zhang, Z. Wang, Y. Yao, X. He, C. Zhang, D. Zhang, Strontium-doped perovskite oxide $La_{1-x}Sr_xMnO_3$ (x=0, 0.2, 0.6) as a highly efficient electrocatalyst for nonaqueous Li-O_2 batteries, Electrochimica Acta, 232 (2017) 296-302.

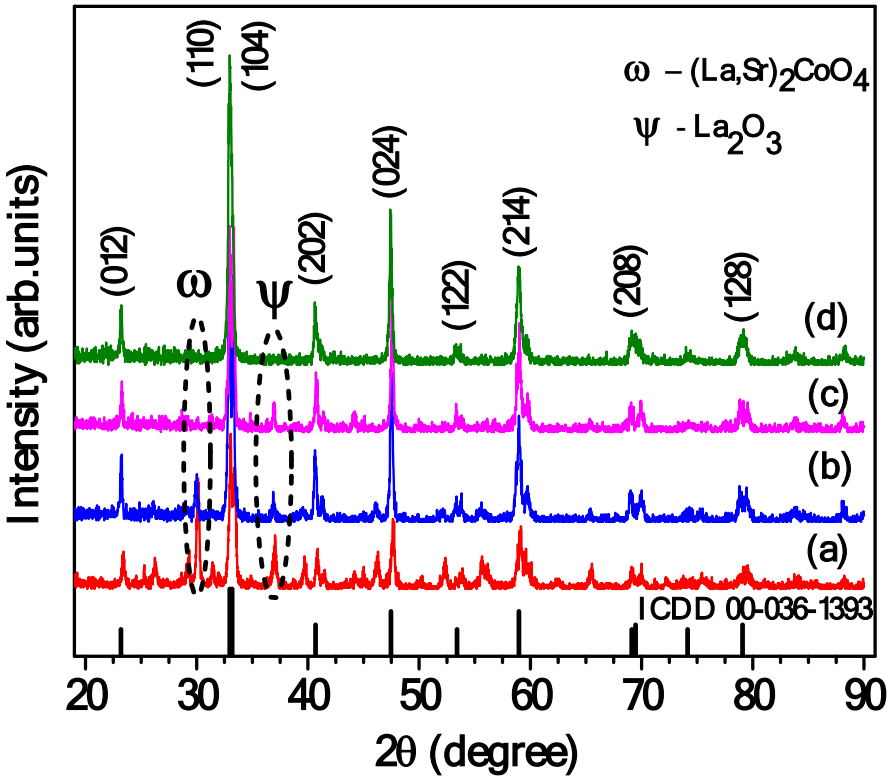

Figure S1. The XRD pattern of the synthesised $La_{0.6}Sr_{0.4}CoO_3$ (HS LSC) at different temperatures (a) 700 °C (HS LSC-7), (b) 800 °C (HS LSC-8), (c) 900 °C (HS LSC-9), and (d) 1000 °C (HS LSC-10).

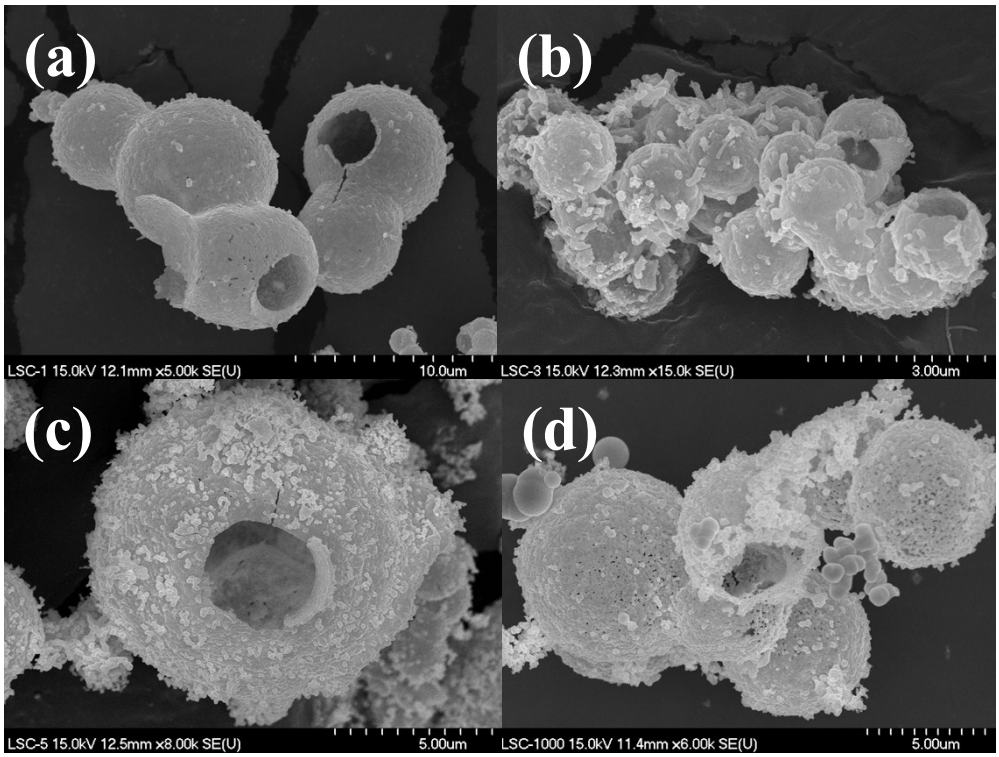

Figure S2. Scanning electron microscope images of pristine HS LSC-7 (a), HS LSC-8 (b), HS LSC-9 (c) and HS LSC-10 (d).

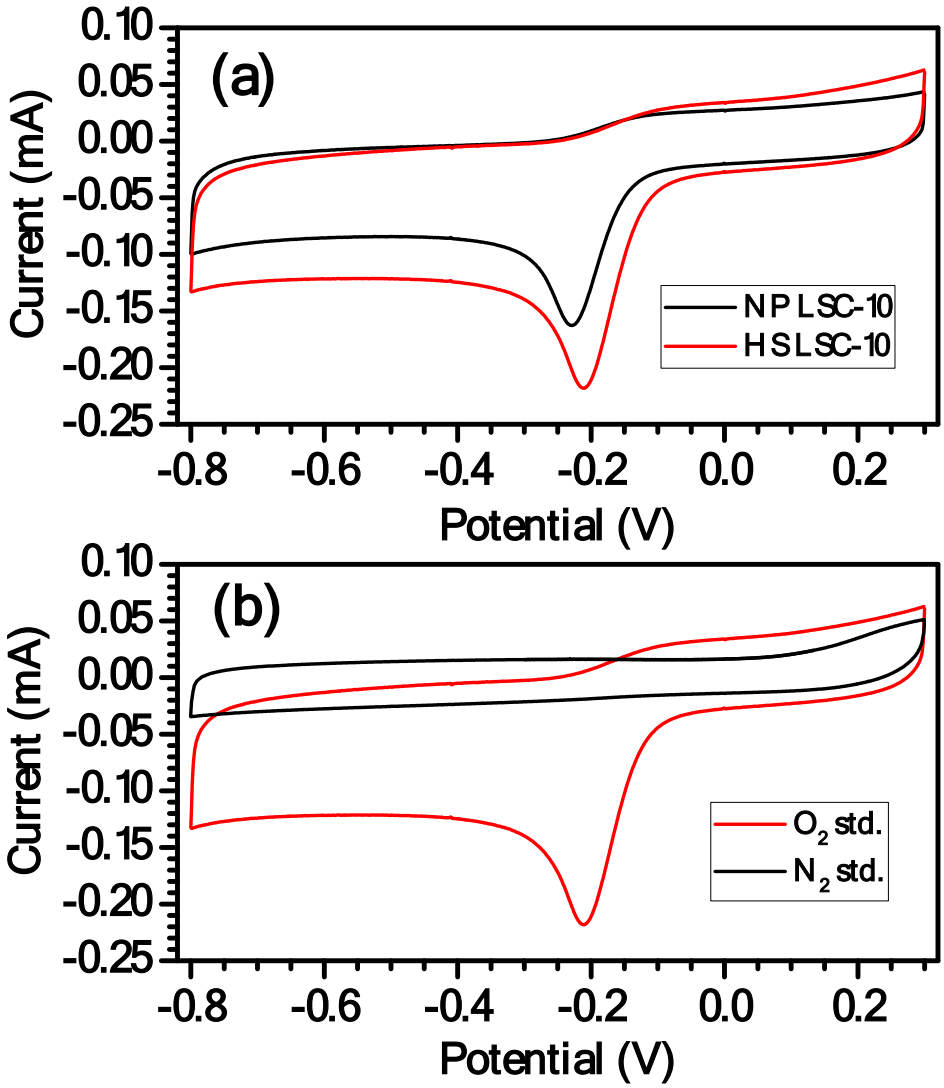

Figure S3. (a) Comparison cyclic voltammetry of NP-LSC-10 and HS-LSC-10 in O_2 saturated 0.1 M KOH electrolyte and (b) comparison CV of HS-LSC-10 in O_2 and N_2 saturated 0.1 M KOH solution at 5 mV s^{-1} scan rate.

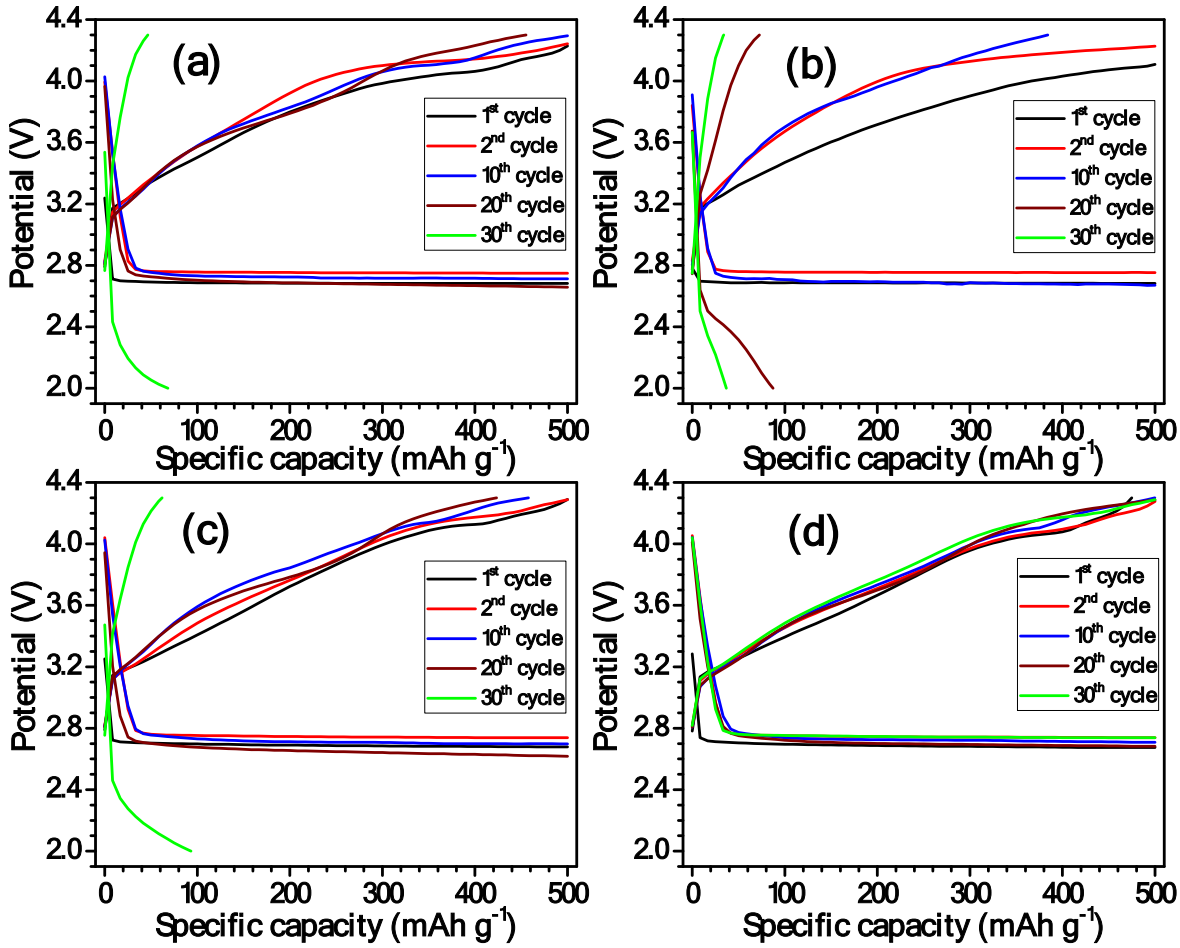

Figure S4. The limited capacity range charge/discharge curves of (a) HS LSC-7, (b) HS LSC-8, (c) HS LSC-9 and (d) HS LSC-10 catalyst at 100 m g^{-1} between 2 to 4.3 V.

Calibration of Hg/HgO reference electrode:

The calibration of Hg/HgO reference electrode was performed in a standard three-electrode system with polished Pt wire as the working and counter electrodes, and the Hg/HgO electrode used as reference electrode. The standard electrode potential of Hg/HgO/1M KOH was 0.118 V *vs.* SHE based on the manufacture's specification (ALS co., Ltd). 0.1 M KOH electrolyte is pre-purged and saturated with high purity H_2 gas for 20 minutes. Linear scanning voltammetry is then run at a scan rate of 0.5 mV s^{-1}, and the potential at which the current crossed zero is taken to be the thermodynamic potential for the hydrogen electrode reactions. Here, the zero-current point is at -0.886 V, so (E(RHE) = E(Hg/HgO) +0.886 V).